The α-Effect and Competing Mechanisms: The Gas-Phase Reactions of Microsolvated Anions with Methyl Formate

ARTICLE *in* JOURNAL OF THE AMERICAN SOCIETY FOR MASS SPECTROMETRY · DECEMBER 2013

Impact Factor: 2.95 · DOI: 10.1007/s13361-013-0781-z · Source: PubMed

J. Am. Soc. Mass Spectrom. (2014) 25:159–168
DOI: 10.1007/s13361-013-0781-z

RESEARCH ARTICLE

The α-Effect and Competing Mechanisms: The Gas-Phase Reactions of Microsolvated Anions with Methyl Formate

Ditte L. Thomsen,[1,2] Charles M. Nichols,[2] Jennifer N. Reece,[2] Steen Hammerum,[1] Veronica M. Bierbaum[2]

[1]Department of Chemistry, University of Copenhagen, Universitetsparken 5, DK-2100, Copenhagen, Denmark
[2]Department of Chemistry and Biochemistry, University of Colorado, 215 UCB, Boulder, CO 80309, USA

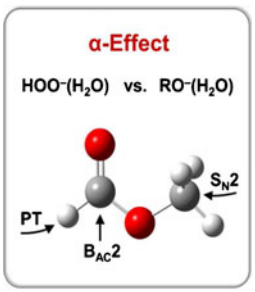

Abstract. The enhanced reactivity of α-nucleophiles, which contain an electron lone pair adjacent to the reactive site, has been demonstrated in solution and in the gas phase and, recently, for the gas-phase S_N2 reactions of the microsolvated $HOO^-(H_2O)$ ion with methyl chloride. In the present work, we continue to explore the significance of microsolvation on the α-effect as we compare the gas-phase reactivity of the microsolvated α-nucleophile $HOO^-(H_2O)$ with that of microsolvated normal alkoxy nucleophiles, $RO^-(H_2O)$, in reactions with methyl formate, where three competing reactions are possible. The results reveal enhanced reactivity of $HOO^-(H_2O)$ towards methyl formate, and clearly demonstrate the presence of an overall α-effect for the reactions of the microsolvated α-nucleophile. The association of the nucleophiles with a single water molecule significantly lowers the degree of proton abstraction and increases the S_N2 and $B_{AC}2$ reactivity compared with the unsolvated analogs. $HOO^-(H_2O)$ reacts with methyl formate exclusively via the $B_{AC}2$ channel. While microsolvation lowers the overall reaction efficiency, it enhances the $B_{AC}2$ reaction efficiency for all anions compared with the unsolvated analogs. This may be explained by participation of the solvent water molecule in the $B_{AC}2$ reaction in a way that continuously stabilizes the negative charge throughout the reaction.

Key words: α-Effect, Reactivity enhancement, Brønsted correlation, Nucleophilic substitution, Acyl substitution, Riveros reaction, Micro-hydration, Ion–molecule reaction, Isotope labeling

Received: 25 July 2013/Revised: 5 November 2013/Accepted: 7 November 2013/Published online: 18 December 2013

Introduction

Studies of gas-phase ion-molecule reactions provide insight into intrinsic reactivity in the absence of counter ions and solvent effects. Drastic differences are observed between gas-phase and condensed-phase reactivity, as demonstrated for the reaction of HO^- with methyl formate for which the gas-phase reaction rate constant exceeds that in solution by about nine orders of magnitude [1]. The controlled addition of solvent molecules to the gas-phase ions, known as microsolvation, allows us to explore the role of solvent and to probe the transition between gas-phase and condensed-phase reactivity.

One area in which the significance of the solvent has been thoroughly examined is the influence of solvent effects on the α-effect [2]. This term describes an enhanced reactivity of nucleophiles that possess an electron lone pair adjacent to the reactive site (e.g., neutral nucleophiles such as hydrazine and hydroxylamine or ionic nucleophiles such as the hydrogen peroxide and hypochlorite anions). In solution, these α-nucleophiles show positive deviation from Brønsted-type correlations relative to normal nucleophiles of similar basicity. The α-effect has been observed in several different types of reactions, including nucleophilic reactions at saturated [3–9] as well as at unsaturated carbon [9–14] and in such diverse solvents as H_2O, DMSO, CH_3CN, and toluene [15]. This has led to an active controversy about whether the α-effect is controlled by intrinsic properties of the α-nucleophile or by external solvent effects.

Large α-effects have been reported for basic nucleophilic ester cleavage in solution; these reactions occur primarily by way of acyl substitution [10–12]. The α-effect has been shown to vary strongly with the local environment of the carbon atom that undergoes nucleophilic attack, as significantly larger α-effects have been reported for reactions at unsaturated carbon atoms than at saturated carbon atoms [15]. Methyl formate features a methyl as well as a carbonyl group, which makes it an ideal substrate for studies of the

Correspondence to: Veronica M. Bierbaum; *e-mail:* veronica.bierbaum@colorado.edu

gas-phase α-effect for nucleophilic attack at both saturated and unsaturated carbon. As shown in Scheme 1, the gas-phase reactions of methyl formate take place via three primary channels: abstraction of the carbonyl proton (PT), nucleophilic substitution at the methyl group (S_N2), and nucleophilic acyl substitution ($B_{AC}2$). The proton transfer reaction, also referred to as the Riveros reaction, is driven by expulsion of CO and formation of an anionic cluster [16]; direct proton transfer would be endothermic.

Gas-phase studies are particularly appropriate when examining the intrinsic nature of the α-effect, and several studies have addressed reactions of nucleophiles with methyl formate in the gas phase [17–22]. The early studies by DePuy et al. [17] compared the gas-phase reactivity of the HOO^- and HO^- anions with methyl formate and found similar reaction efficiencies and product distributions ($PT:S_N2:B_{AC}2$) for the reactions of HOO^- (64 %:8 %:28 %) and HO^- (61 %:5 %:34 %), respectively. The authors concluded that the presence of a gas-phase α-effect was not obvious; however, this was subsequently questioned, since the basicity of HO^- far exceeds that of HOO^-, and similar behavior would imply enhance reactivity of the α-nucleophile [23]. Also, more pronounced single-electron-transfer in the HOO^- transition state led Patterson and Fountain [23] to support the presence of an α-effect. A recent gas-phase study by Garver et al. [20] extended the series of nucleophiles to include CD_3O^-, $CH_3CD_2O^-$, and i-$C_3H_7O^-$, as well as HO^- and HOO^-. The reaction rate constants were similar and approaching the collision rate constant for all nucleophiles; no overall α-effect could be observed. However, the results clearly demonstrated the presence of a gas-phase α-effect in both the S_N2 and the $B_{AC}2$ reaction channels. Surprisingly, the effect was of similar magnitude in both channels, even though significantly larger α-effects have been reported for condensed-phase reactions at unsaturated carbon [15]. Besides methyl formate, other substrates with competing reaction pathways have been employed to study the gas-phase α-effect [20, 24, 25]. McAnoy et al. [24] compared the gas-phase reactivity of HOO^- to that of CH_3O^- in reactions with dimethyl methylphosphonate and report an α-effect based on major differences in product distribution. While CH_3O^- reacts almost exclusively via proton abstraction (97 %), HOO^- reacts primarily via the S_N2 pathway (89 %) and, thus, exhibits enhanced carbon nucleophilicity.

Having established the presence of an α-effect in the gas-phase reaction with methyl formate, a natural next step is to consider how solvent influences the effect. That the α-effect is influenced by solvent effects was shown in recent studies of the S_N2 reactions of microsolvated anions with methyl chloride, which demonstrated that associating the anions with just a single water molecule allowed observation of an α-effect, which was not apparent in the studies of the reactions of unsolvated anions with methyl chloride [26]. Similarly, studies of anions solvated with methanol revealed enhanced reactivity of α-nucleophiles [27].

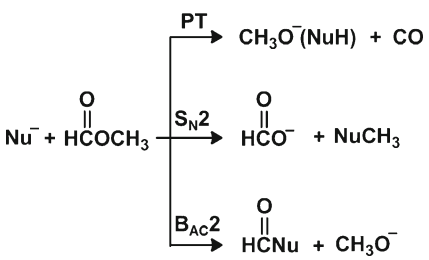

Scheme 1. Competing mechanisms in the nucleophilic reaction with methyl formate

In the present study, we investigate the α-nucleophilicity of the microsolvated hydrogen peroxide anion, $HOO^-(H_2O)$, and report overall rate constants and reaction efficiencies along with product distributions for the gas-phase reactions of HOO^-, $H^{18}O^-$, CD_3O^-, $CH_3CD_2O^-$, and i-$C_3H_7O^-$ with methyl formate in the presence of a single water molecule. Oxygen-18 and deuterium labeling were employed where necessary to distinguish among the different product channels. The influence of the α-effect on the reactions of the microsolvated $HOO^-(H_2O)$ is demonstrated by comparing the reaction efficiency to that of the microsolvated normal nucleophiles. The α-effect is evaluated for the overall reaction efficiency as well as for the efficiency corresponding to the specific reactions channels.

Experimental

The experiments were carried out with a flowing afterglow-selected ion flow tube (FA-SIFT) instrument, which has been described previously [28, 29]. Briefly, ions are produced in a flowing afterglow ion source and mass-selected using a quadrupole mass filter prior to injection into a reaction flow tube. HO^- was prepared by electron ionization (70 eV) of traces of methane and nitrous oxide in helium buffer gas. HOO^- was generated by proton abstraction from H_2O_2 by NH_2^-, which was prepared by electron ionization of NH_3. All other anions were formed by proton abstraction of the corresponding neutrals by HO^-. The microsolvated ions were prepared by introducing a mixture of H_2O in tetrahydrofuran slightly downstream of the production of bare ions. In previous studies, tetrahydrofuran was shown to enhance the formation of microsolvated ions [30]. The mass-selected ions are injected into the reaction flow tube through a Venturi inlet and entrained in a flow of helium (~0.5 Torr); thousands of collisions with the buffer gas insure a thermal energy distribution of the reactant ions prior to reaction with the neutral reagent. A known flow of neutral reagent is added through a manifold of inlets along the reaction flow tube, and finally, ionic reagents and products are analyzed using a quadrupole mass filter coupled to an electron multiplier.

The decrease in reactant ion signal is measured as a function of reaction distance (which is directly proportional to the reaction time), and a rate constant is derived assuming pseudo first-order kinetics. All reported reaction rate constants and product distributions represent the average of at least three individual measurements. Reaction efficiencies

are the ratio between the experimental rate constant (k_{exp}) and the collision rate constant (k_{col}), calculated from parameterized trajectory collision rate theory [31]. Product distributions are determined by extrapolating the product fractions to zero reaction time to eliminate secondary reactions and differential diffusion effects. The product distributions were corrected for reaction of the bare ion, which was always present as a result of collision-induced dissociation upon injection of the microsolvated ion into the reaction flow tube. Mass discrimination was minimized and not considered further. Absolute uncertainties are ±30 % with respect to the rate constants and ±50 % with respect to the product distributions attributable to uncertainties in pressure, flow, and temperature. All reagents were obtained from commercial sources and used without further purification: hydrogen peroxide (H_2O_2, Sigma-Aldrich, 50 wt.% solution in water); water-d_2 (D_2O, Cambridge Isotope, Tewksbury (MA), USA, 99.9 % D); water-^{18}O (H_2O^{18}, Cambridge Isotope, 97 % ^{18}O); methanol-d_4 (CD_3OD, CDN Isotopes, 99.8 % D); ethyl-1,1-d_2 alcohol (CH_3CD_2OH, Aldrich, 98 % D); 2-propanol (i-C_3H_7OH, Fisher Scientific, 99.9 %); methyl formate (CH_3OCHO, Sigma Aldrich, 99 %); tetrahydrofuran (THF, Sigma Aldrich, 99.9 %); ammonia (NH_3, Airgas, 99.9995 %). Helium buffer gas (He, Airgas, 99.995 %) was purified by passage through a molecular sieve trap immersed in liquid nitrogen.

Computational

All calculations were carried out with the Gaussian 09 program [32]. Equilibrium and transition state structures were localized as stationary points on the potential energy surface. Structures were optimized at the MP2/6-311++G(d,p) level of theory. Harmonic vibrational frequencies were obtained at the same level and used to verify the nature of the stationary points as minima and first order saddle points, respectively. Thermochemical properties were calculated using a modified version of the composite G3 method, in which all geometry optimizations and harmonic vibrational frequency calculations were carried out with the 6-31+G(d) basis set instead of the default 6-31G(d). The diffuse functions are included to allow a better description of the anions. This treatment is comparable to the G2(+) method, which has been successfully employed in previous studies of reactions involving anions [33, 34]. To obtain zero-point energies and thermal corrections, the harmonic frequencies were scaled by a factor of 0.8929 as implemented in the G3 method. Use of the scaling factor of 0.8970 proposed by Scott and Radom [35] gave no significant changes to the thermochemical properties. Proton affinities (PA) of the microsolvated nucleophiles correspond to the calculated reaction enthalpies at 298 K:

$$Nu^-(H_2O) + H^+ \rightarrow NuH(H_2O) \quad (1)$$

Results and Discussion

Reaction Efficiencies

The rate constants and reaction efficiencies measured for the reactions of microsolvated anions with methyl formate are displayed in Table 1, together with the calculated proton affinities of the microsolvated nucleophiles. The overall rate constant is derived from the observed depletion in the microsolvated reactant ion signal and, hence, includes contributions from all three competing reaction channels. Figure 1 shows a Brønsted-type plot of the reaction efficiency versus the proton affinity of the microsolvated anion. Efficiencies for reactions of the unsolvated nucleophiles are included for comparison. It is evident from the plot that the reaction efficiency of the $HOO^-(H_2O)$ cluster stands out from the rate–energy relationship found for the normal microsolvated nucleophiles. The enhanced reactivity of the microsolvated hydrogen peroxide anion clearly demonstrates the presence of an α-effect in the reaction with methyl formate.

Incremental microsolvation has previously been shown to rapidly decrease the reaction efficiency of substitution at saturated carbon centers [36–41]. In a recent study involving the same series of microsolvated anions reacting with methyl chloride, we demonstrated a decrease in reaction efficiency of up to a factor of 100 upon attachment of a single water molecule [26]. Interestingly, the reaction efficiency with methyl formate is much less affected by the water molecule, as the decrease is at most a factor of six. It is particularly striking that the $HO^-(H_2O)$ cluster shows the same reaction efficiency as the unsolvated HO^- ion, and that the $HOO^-(H_2O)$ cluster reacts with an efficiency of 0.45, only slightly less than the 0.61 observed for the unsolvated HOO^- ion. The effect of the water molecule on the reaction efficiency increases with increasing size of the alkoxy moiety, from $CD_3O^-(H_2O)$ to i-$C_3H_7O^-(H_2O)$. Even though microsolvation results in a decrease in efficiency, the effect is not as drastic as that observed for attack on saturated substrates. This could be due to interaction of the water molecule with the carbonyl group in the transition state, vide infra.

The reaction efficiencies of the unsolvated nucleophiles are all large and quite similar (between 0.61 and 0.65). When the nucleophile is associated with a single water molecule, a reactivity difference arises across the series of nucleophiles (Figure 1). It has been suggested that there is a direct relationship between the magnitude of the α-effect and the Brønsted β_{nuc} parameter (the slope of a Brønsted plot) [4]. Furthermore, it has been argued that the β_{nuc} value reflects the amount of single-electron-transfer (SET) in the transition state [42–44], and that enhanced SET character would be directly related to a larger α-effect [23, 45]. The Brønsted plot shown in Figure 1 yields the β_{nuc} values for reactions of the unsolvated and microsolvated nucleophiles, and even though the data for the microsolvated nucleophiles exhibit some deviation from a straight line, a qualitative comparison demonstrates that the β_{nuc} value for the microsolvated nucleophiles is much larger than the β_{nuc}

Table 1. Kinetic Data, Product Distributions, and Thermodynamic Data for Reaction of Microsolvated Anions with Methyl Formate: $Nu^-(H_2O)+CH_3OCHO$

	PA[a]	Kinetic data[b]		PT		S_N2		$B_{AC}2$	
		k_{exp} (x 10^{-10})	Eff	$\%_{PT}$ (Eff) [c]	$\Delta H^{\ddagger d}$	$\%_{SN2}$ (Eff) [c]	$\Delta H^{\ddagger d}$	$\%_{BAC2}$ (Eff) [c]	$\Delta H^{\ddagger d}$
$HO^-(H_2O)$	1538	13.9±0.3	0.64	50 % (0.32)	−51	-	−2	50 %[e] (0.32)	−48
$CD_3O^-(H_2O)$	1527	6.4±0.2	0.33	20 % (0.07)	−47	40 % (0.13)	−3	40 % (0.13)	−44
$CH_3CD_2O^-(H_2O)$	1517	4.0±0.1	0.22	25 % (0.06)	−41	65 % (0.14)	3	10 % (0.02)	−43
i-$C_3H_7O^-(H_2O)$	1505	1.8±0.1	0.10	40 % (0.04)	−38	60 % (0.06)	8	-	−40
$HOO^-(H_2O)$	1493	8.7±0.1	0.45	-	−38	-	1	100 %(0.45)	−45

[a]Proton affinities of the microsolvated anions in units of kJ/mol are calculated using a modified version of the composite G3 method
[b]Overall rate constant (k_{exp}) in units of cm^3 $molecule^{-1}$ s^{-1}. Error bars represent one standard deviation, absolute uncertainty is ±30 %. Reaction efficiency (Eff) is the ratio of the overall rate constant (k_{exp}) and the collision rate constant (k_{col})
[c]Product distributions are determined by extrapolating the product fractions to zero reaction time; absolute uncertainty is ±50 %. Eff for each reaction mechanism is determined as the overall reaction efficiency multiplied by the product distribution, i.e. $Eff_{BAC2} = Eff_{Total} \bullet \%_{BAC2}$
[d]Transition state enthalpies ($\Delta H^{\ddagger}$) in units of kJ/mol are calculated using a modified version of the composite G3 method
[e]Fifty percent provides an upper limit to the $B_{AC}2$ channel

value for the unsolvated nucleophiles. The drastic change of the β_{nuc} value upon microsolvation tallies well with the experimental finding that there is no apparent overall α-effect for the unsolvated nucleophiles, whereas the α-effect strongly influences the reactions when even a single water molecule is present. Microsolvation allows the α-effect to be observed in a manner similar to that found for the reactions with methyl chloride [26]. The attachment of just a single water molecule would appear to mimic the early stages of solvation, particularly the reactivity enhancement observed for the hydrogen peroxide anion in solution.

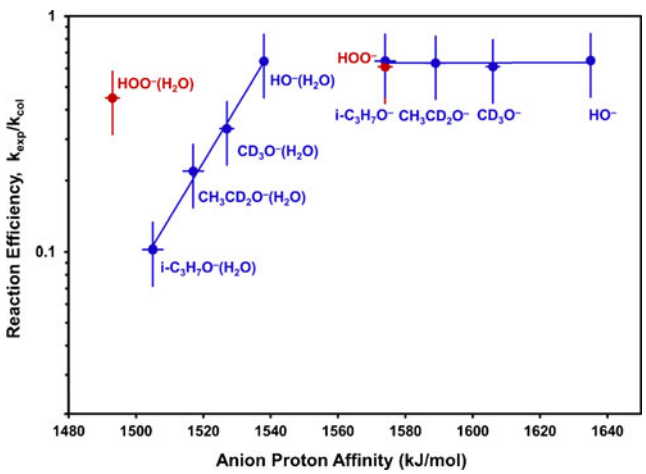

Figure 1. Reaction efficiency (k_{exp}/k_{col}) versus anion proton affinity (PA) for the reactions of unsolvated and microsolvated anions with methyl formate. Normal nucleophiles are displayed in blue and α-nucleophiles in red. The trend lines are fits to the unsolvated and microsolvated normal nucleophile data sets. Reaction efficiencies for the unsolvated anions are obtained from Reference [20]. The anion proton affinity is calculated using a modified version of the composite G3 method. The vertical error bars represent the absolute uncertainty of ±30 %. The horizontal error bars represent the experimental uncertainty in the proton affinity of the bare ion, against which the computed PAs are benchmarked

Product Distributions

The product distributions ($PT:S_N2:B_{AC}2$) for the microsolvated nucleophiles are shown in Table 1. The presence of a water molecule results in a more complex product ion distribution than observed for the unsolvated nucleophiles, as the possibility of clustering of the product ions with the water molecule increases the number of available product channels. Determining product distributions, therefore, becomes increasingly challenging, and product distributions are reported to the nearest 5 %. In the following section, the product distributions for reaction of the microsolvated alkoxy anions, $RO^-(H_2O)$, the $HO^-(H_2O)$ cluster, and the $HOO^-(H_2O)$ cluster are described in detail.

Scheme 2 summarizes the product formation for reactions of the microsolvated alkoxy anions. An intriguing observation is that the $CH_3O^-(ROH)$ cluster is definitively observed as a product in the reactions of all three alkoxy cluster ions, even though the direct formation in the PT transfer channel would be endothermic. We therefore propose that the $CH_3O^-(ROH)(H_2O)$ ions are first formed in exothermic PT processes, and then dissociate by multiple collisions with helium at room temperature. Dissociation likely occurs by the lowest energy pathway that corresponds to loss of H_2O rather than ROH. The formation of the $CH_3O^-(H_2O)$ product cluster presumably occurs by the near-thermoneutral $B_{AC}2$ reaction for $CD_3O^-(H_2O)$ and $CH_3CD_2O^-(H_2O)$, but is absent in the corresponding endothermic reaction of i-$C_3H_7O^-(H_2O)$. The resulting product distribution ($PT:S_N2:B_{AC}2$) for the reactions of $CD_3O^-(H_2O)$ is (20 %:40 %:40 %), for $CH_3CD_2O^-(H_2O)$ it is (25 %:65 %:10 %), and for i-$C_3H_7O^-(H_2O)$ it is (40 %:60 %:0 %). The reactivity of the microsolvated alkoxy anions differ mostly in the $B_{AC}2$

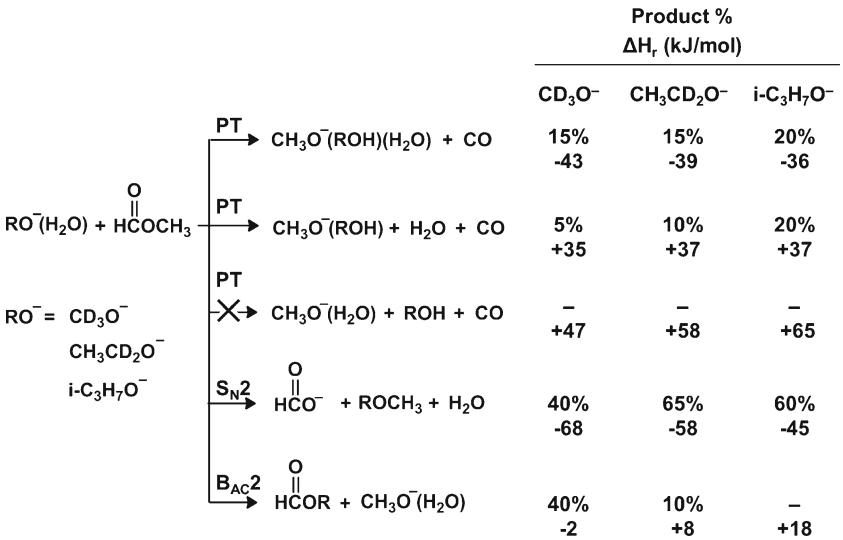

Scheme 2. Product ion distribution and calculated reaction enthalpies for the reaction of microsolvated alkoxy anions with methyl formate. Formation of $CH_3O^-(ROH)$ does not occur by the endothermic PT reaction but rather by collisional dissociation of $CH_3O^-(ROH)(H_2O)$

channel, in which the reaction efficiency decreases rapidly in going from $CD_3O^-(H_2O)$ to i-$C_3H_7O^-(H_2O)$. The latter does not show any $B_{AC}2$ reactivity, which is reasonable since i-$C_3H_7O^-(H_2O)$ is a better leaving group than $CH_3O^-(H_2O)$, and the collapse of the tetrahedral intermediate could well lead to loss of the attacking i-$C_3H_7O^-(H_2O)$ rather than of the $CH_3O^-(H_2O)$ moiety.

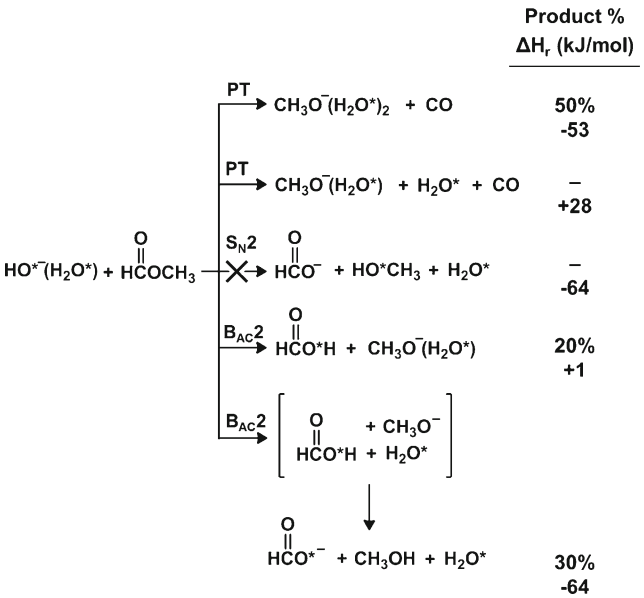

Scheme 3. Product ion distribution and calculated reaction enthalpies for the reaction of $HO^-(H_2O)$ with methyl formate. An asterisk denotes oxygen-18 labeling. The product $CH_3O^-(H_2O^*)$ is assigned to the $B_{AC}2$ rather than PT mechanism

Scheme 3 summarizes the product formation for the reactions of $HO^-(H_2O)$; an asterisk denotes oxygen-18 labeling. Labeling was employed to distinguish the S_N2 product ion ($HC(O)O^-$) from that of the $B_{AC}2$ product ion ($HC(O)O^{*-}$). The unlabeled formate ion, $HC(O)O^-$, is not observed as a product, demonstrating that the S_N2 reaction does not take place. In addition to the PT and $B_{AC}2$ channels described for the alkoxy anions, the $HO^-(H_2O)$ cluster has an additional $B_{AC}2$ channel in which proton transfer occurs within the product complex of the $B_{AC}2$ pathway. This is demonstrated by the formation of the oxygen-18-labeled formate ion, $HC(O)O^{*-}$, which arises via proton transfer from the initially formed formic acid. Earlier studies of the $B_{AC}2$ reaction for nucleophiles such as HO^-, HOO^-, and NH_2^- in gas-phase reactions with methyl formate have demonstrated similar proton transfer processes [18–21].

The $CH_3O^-(H_2O^*)$ product ion ascribed to the $B_{AC}2$ channel could also be formed in the PT channel as discussed for the microsolvated alkoxy anions. It is likely that the $CH_3O^-(H_2O^*)$ product ion does not solely arise from the $B_{AC}2$ reaction pathway; some could be formed via dissociation of the ternary $CH_3O^-(H_2O^*)_2$ product ion cluster of the PT pathway, upon collision with helium. Since we cannot monitor the neutral products, we are unable to distinguish between the contributions from the two channels. For the present study, we cautiously assign the $CH_3O^-(H_2O^*)$ product ion to the $B_{AC}2$ channel based on the more favorable reaction enthalpy of this pathway. The resulting product distribution (PT:S_N2:$B_{AC}2$) for reaction of the $HO^-(H_2O)$ cluster is (50 %:0 %:50 %), with 50 % providing an upper limit to the $B_{AC}2$ channel. Direct dynamics

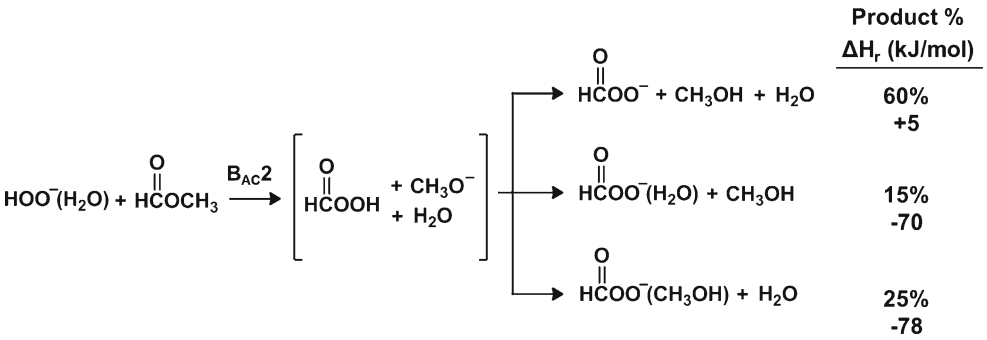

Scheme 4. Product ion distribution and calculated reaction enthalpies for the reaction of $HOO^-(H_2O)$ with methyl formate

simulations would be valuable in providing a better understanding of this product distribution [46, 47].

Scheme 4 summarizes the product formation for the reactions of $HOO^-(H_2O)$. The hydrogen peroxide anion is structurally quite similar to the hydroxide anion, and the $HOO^-(H_2O)$ also forms an initial $B_{AC}2$ product that may undergo subsequent proton transfer. In fact, the $HOO^-(H_2O)$ cluster reacts with methyl formate exclusively via the $B_{AC}2$ channel. We see formation of the performate ion, $HC(O)O_2^-$, and the clusters $HC(O)O_2^-(H_2O)$ and $HC(O)O_2^-(CH_3OH)$, all of which arise via proton transfer within the product complex of the $B_{AC}2$ pathway. We have recently shown that the structure of the microsolvated $HOO^-(H_2O)$ cluster resembles $HO^-(HOOH)$, but that HOO^- is still the active nucleophile when the cluster ion reacts [26]. Formation of $HC(O)O_2^-$ and clusters of this ion in the reaction with methyl formate provide additional evidence that HOO^- is the nucleophilic part of the $HOO^-(H_2O)$ cluster.

Comparison of the product distributions for the microsolvated anions with those of the unsolvated analogs (Table 2) reveals that attachment of a single water molecule significantly lowers the degree of proton abstraction and increases the S_N2 and $B_{AC}2$ reactivity. A disfavoring of proton abstraction compared with nucleophilic attack on carbon has previously been ascribed to lowering of the anion basicity upon solvation [1].

Table 2. Proton Affinities, Reaction Efficiencies, and Product Distributions for Reaction of the Unsolvated Anions with Methyl formate: Nu^-+CH_3OCHO

	PA[a]	Eff[b]	PT (Eff)[b]	S_N2 (Eff)[b]	$B_{AC}2$ (Eff)[b]
$H^{18}O^-$	1635	0.65	59 % (0.38)	8 % (0.05)	33 % (0.21)
CD_3O^-	1606	0.61	79 % (0.48)	3 % (0.02)	18 % (0.11)
$CH_3CD_2O^-$	1589	0.63	97 % (0.61)	<1 %	3 % (0.02)
i-$C_3H_7O^-$	1574	0.64	100 % (0.64)	-	-
HOO^-	1574	0.61	64 % (0.39)	8 % (0.05)	28 % (0.17)

[a]Proton affinities of the anions in units of kJ/mol are calculated using a modified version of the composite G3 method
[b]Reaction efficiencies (Eff) and product distributions from Reference [20]; Eff in parentheses for each reaction mechanism, determined as the overall reaction efficiency multiplied by the product distribution (i.e., $Eff_{BAC2} = Eff_{Total} \bullet \%_{BAC2}$)

Figure 2 displays representative structures of the optimized transition states for the attack leading to the PT, S_N2, and $B_{AC}2$ reactions, respectively. Calculated transition state enthalpies are shown in Table 1. A striking feature of the transition state enthalpies is that the S_N2 process is able to compete with proton transfer for the three microsolvated alkoxy anions despite the high transition state enthalpies calculated for the S_N2 reactions relative to the PT reactions. Examination of the optimized transition state structures in Figure 2 reveals that the PT requires a highly ordered transition state in which the water molecule interacts with the carbonyl oxygen. In the investigations of HOO^- and CH_3O^- reacting with dimethyl methylphosphonate, McAnoy et al. [24] estimated pre-Arrhenius factors that favor S_N2 reaction over the PT channel. Similarly, the observed preference for the S_N2 pathway in the current reactions with methyl formate might be attributed to entropic contributions.

Two points can be made about the calculated $B_{AC}2$ transition state enthalpies. First, the $B_{AC}2$ reaction barrier of $HOO^-(H_2O)$ attack is similar in magnitude to those of the microsolvated normal nucleophiles, suggesting that the exclusive preference for $B_{AC}2$ attack of $HOO^-(H_2O)$ is not due to significantly different barrier heights. Second, despite a very low transition state enthalpy of $B_{AC}2$ reaction for all microsolvated nucleophiles, this reaction pathway is disfavored for the $C_2H_5O^-$ and i-$C_3H_7O^-$ anions, probably due to the overall endothermicity of the reactions. As discussed previously, it is energetically more advantageous to lose the attacking $RO^-(H_2O)$ rather than the $CH_3O^-(H_2O)$ moiety upon collapse of the tetrahedral intermediate.

$B_{AC}2$ Reaction Efficiency

Table 1 displays the specific efficiencies of each reaction channel determined as the overall reaction efficiency multiplied by the product distribution (i.e., $Eff_{BAC2} = Eff_{Total} \bullet \%_{BAC2}$). By means of the specific reaction efficiencies, we can evaluate the α-effect for each of the reaction channels that involve nucleophilic attack on a

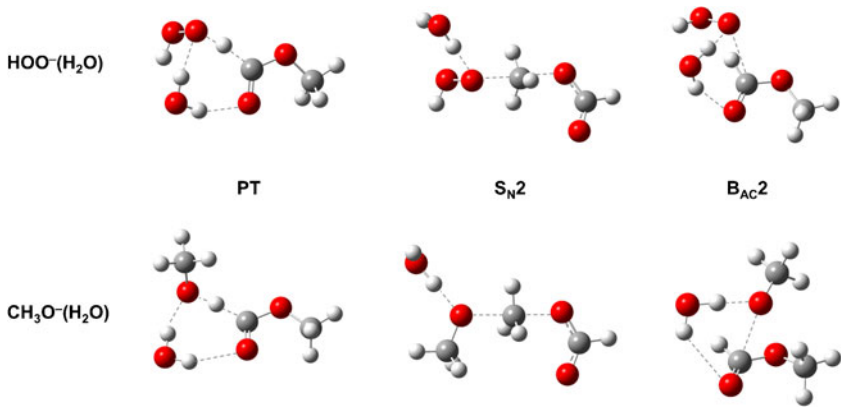

Figure 2. Calculated transition state structures for the attack leading to PT, S_N2, and $B_{AC}2$ reaction, respectively, in the reaction of methyl formate with $HOO^-(H_2O)$ and $CH_3O^-(H_2O)$. Optimized at the MP2/6-311++G(d,p) level of theory

carbon atom, namely the S_N2 and $B_{AC}2$ reactions. The α-effect is assessed by comparison of the specific efficiencies corresponding to the $HOO^-(H_2O)$ cluster with those of the microsolvated normal nucleophiles. Since $HOO^-(H_2O)$ reacts exclusively by attack on the carbonyl carbon, the α-effect can only be evaluated for the $B_{AC}2$ channel. The reported $B_{AC}2$ efficiency for the $HO^-(H_2O)$ cluster provides an upper limit to the efficiency since the product distribution provides only an upper limit to the $B_{AC}2$ channel, as previously discussed.

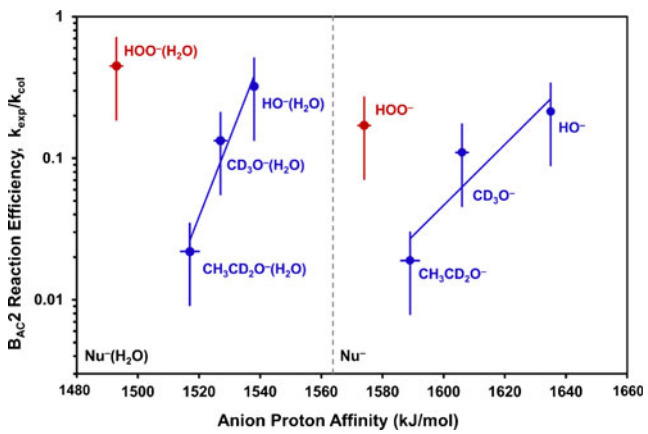

Figure 3. $B_{AC}2$ reaction efficiency (k_{exp}/k_{col}) versus anion proton affinity (PA) for the reactions of unsolvated and microsolvated anions with methyl formate. Normal nucleophiles are displayed in blue and α-nucleophiles in red. The $B_{AC}2$ reaction efficiency is determined as the overall reaction efficiency multiplied by the product distribution (i.e., $Eff_{BAC2} = Eff_{Total} \bullet \%_{BAC2}$). Reaction efficiencies for the unsolvated anions are obtained from Reference [20]. The anion proton affinity is calculated using a modified version of the composite G3 method. The vertical error bars represent the combined uncertainty of the rate constant and the product distribution. The horizontal error bars represent the experimental uncertainty in the proton affinity of the bare ion, against which the computed PAs are benchmarked

Figure 3 shows a Brønsted-type plot of the $B_{AC}2$ reaction efficiency versus the proton affinity of the microsolvated anions. $B_{AC}2$ efficiencies for reaction of the unsolvated nucleophiles are included for comparison. The results summarized in Figure 3 clearly illustrate that $HOO^-(H_2O)$, despite the lower proton affinity, has the largest $B_{AC}2$ efficiency observed for any of the microsolvated nucleophiles and, thereby, demonstrates the presence of a substantial α-effect in the $B_{AC}2$ reaction with methyl formate.

Garver et al. [20] have demonstrated that the unsolvated HOO^- anion shows an α-effect in the $B_{AC}2$ reaction with methyl formate, and the present results demonstrate that the attachment of a single water molecule enhances the effect.

As described above, the $HOO^-(H_2O)$ cluster reacts via subsequent proton transfer in the $B_{AC}2$ reaction complex, and it is pertinent to consider if this proton transfer is responsible for the $B_{AC}2$ reactivity enhancement of the α-nucleophile. Of the normal nucleophiles, only $HO^-(H_2O)$ forms an initial $B_{AC}2$ product, which undergoes subsequent proton transfer in the same manner as $HOO^-(H_2O)$, and direct comparison of the $B_{AC}2$ reactivity for these two nucleophiles demonstrates that the subsequent proton transfer is not responsible for the observed α-effect. We obtain a $B_{AC}2$ reaction efficiency for $HOO^-(H_2O)$ of 0.45 compared with an upper limit of 0.32 for $HO^-(H_2O)$. Despite the considerably greater proton affinity of the $HO^-(H_2O)$ cluster, the α-nucleophile $HOO^-(H_2O)$ displays the larger reactivity towards the carbonyl carbon. This enhanced reactivity cannot be ascribed to differences between the reaction mechanisms, as both nucleophiles exhibit proton abstraction within the $B_{AC}2$ reaction complex. The result is unambiguous: the enhanced carbonyl reactivity of the $HOO^-(H_2O)$ cluster apparent in Figure 3 originates from an enhanced carbonyl carbon nucleophilicity of the α-nucleophile, not from variations in the $B_{AC}2$ mechanism.

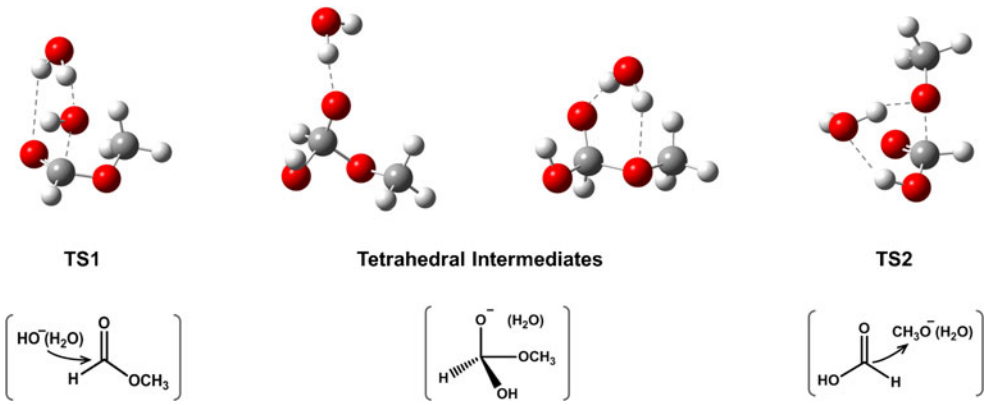

Figure 4. Stationary points along the $B_{AC}2$ reaction pathway of the reaction of $HO^-(H_2O)$ with methyl formate. Optimized at the MP2/6-311++G(d,p) level of theory. The stationary points comprise the transition state of an initial nucleophilic attack (TS1), tetrahedral intermediates, and a final transition state in which the solvated methoxy group is expelled (TS2)

The Brønsted type plot in Figure 3 reveals that attachment of a water molecule uniformly results in enhanced $B_{AC}2$ reaction efficiency, even though the proton affinities are significantly lowered upon microsolvation. This may suggest that the solvent water molecule participates in the $B_{AC}2$ reaction in an entirely different way from that previously found for reaction at saturated carbon [26]. Upon formation of the tetrahedral intermediate, the negative charge is displaced from the attacking nucleophile towards the carbonyl oxygen, and in the subsequent breakdown of the intermediate, the charge shifts to the methoxy leaving group. Figure 4 shows the calculated structures of representative stationary points along the $B_{AC}2$ reaction coordinate for the reaction of the $HO^-(H_2O)$ cluster, illustrating that the water molecule is mobile within the complex and continuously stabilizes the negative charge. The tetrahedral intermediates shown in Figure 4 represent the structures connected to the transitions states through intrinsic reaction coordinate calculations. In a system with multiple hydrogen bond donors and acceptors, there will most likely be several additional conformers of the intermediate.

Conclusions

The gas-phase reactions of microsolvated oxygen centered anions with methyl formate support the premise that an α-effect influences the reactions of microsolvated HOO^- anions. Association of the anions with just a single water molecule results in a reactivity difference across the series of nucleophiles and leads to larger Brønsted β_{nuc} values for the microsolvated nucleophiles compared to the unsolvated analogs. The magnitude of the α-effect is directly related to the magnitude of the β_{nuc} value and, accordingly, we find that the reactions of the microsolvated anions display an overall α-effect with methyl formate, whereas the reactions of the unsolvated anions do not.

Comparison of the product distributions for the microsolvated anions to those of the unsolvated analogs reveals that attachment of a single water molecule significantly lowers the degree of proton abstraction and increases the S_N2 and $B_{AC}2$ reactivity. The effect is particularly pronounced for the microsolvated α-nucleophile, $HOO^-(H_2O)$, which reacts with methyl formate exclusively via the $B_{AC}2$ channel.

The α-effect was evaluated specifically for the $B_{AC}2$ reaction channel to demonstrate that $HOO^-(H_2O)$, despite the lower proton affinity, has the largest $B_{AC}2$ efficiency observed for any of the microsolvated nucleophiles, which demonstrates the presence of a substantial α-effect in the $B_{AC}2$ reaction with methyl formate. Although the overall reaction efficiency is lowered upon the attachment of a water molecule, the $B_{AC}2$ reaction efficiency is enhanced for all anions compared with the unsolvated analogs. The reason may be that the solvent water molecule participates in the $B_{AC}2$ reaction in a way that continuously stabilizes the negative charge throughout the reaction.

Basic ester cleavage in solution occurs predominately by reaction at the carbonyl carbon, and it has been well established that larger α-effects are found for reaction at unsaturated carbons than at saturated sites [15]. The present study of gas-phase microsolvated anions demonstrates how even a single water molecule brings us closer to solution-like reactivity with enhanced preference for nucleophilic reaction at the carbonyl carbon and an increase in the magnitude of the α-effect.

Acknowledgments

The authors gratefully acknowledge NSF (CHE-1012321 and CHE-1300886) for their support of the research. D.L.T thanks the Danish Chemical Society and the Augustinus Foundation, C.M.N. thanks the AFOSR, and J.N.R. thanks the Colorado Diversity Initiative for financial support.

References

1. Pliego, J.R., Riveros, J.M.: The gas-phase reaction between hydroxide ion and methyl formate: a theoretical analysis of the energy surface and product distribution. Chem Eur J **7**, 169–175 (2001)
2. Edwards, J.O., Pearson, R.G.: Factors determining nucleophilic reactivity. J Am Chem Soc **84**, 16–24 (1962)
3. Buncel, E., Wilson, H., Chuaqui, C.: Reactivity selectivity correlations. IV. The α-effect in S_N2 reactions at sp^3 carbon—the reactions of hydrogen-peroxide anion with methyl phenyl sulfates. J Am Chem Soc **104**, 4896–4900 (1982)
4. Dixon, J.E., Bruice, T.C.: α-Effect. V. Kinetic and thermodynamic nature of the α-effect for amine nucleophiles. J Am Chem Soc **94**, 2052–2056 (1972)
5. Fountain, K.R., Dunkin, T.W., Patel, K.D.: α-Effect with substituted *N*-methylbenzohydroxamates and substituted phenyldimethylsulfonium salts: toward understanding of an intrinsic α-effect. J Org Chem **62**, 2738–2741 (1997)
6. Fountain, K.R., Felkerson, C.J., Driskell, J.D., Lamp, B.D.: The α-effect in methyl transfers from S-methyldibenzothiophenium fluoroborate to substituted N-methylbenzohydroxamates. J Org Chem **68**, 1810–1814 (2003)
7. Gregory, M.J., Bruice, T.C.: α-Effect. II. Displacements on sp^3-carbon. J Am Chem Soc **89**, 4400–4402 (1967)
8. McIsaac Jr., J.E., Subbaram, L.R., Subbaram, J., Mulhausen, H.A., Behrman, E.J.: Nucleophilic reactivity of peroxy anions. J Org Chem **37**, 1037–1041 (1972)
9. Fina, N.J., Edwards, J.O.: The α-effect. A review. Int J Chem Kinet **5**, 1–23 (1973)
10. Jencks, W.P., Carriuolo, J.: Reactivity of Nucleophilic reagents towards esters. J Am Chem Soc **82**, 1778–1786 (1960)
11. Bruice, T.C., Donzel, A., Huffman, R.W., Butler, A.R.: Aminolysis of phenyl acetates in aqueous solutions. VII. Observations on influence of salts, amine structure, and base strength. J Am Chem Soc **89**, 2106–2121 (1967)
12. Nomura, Y., Kubozono, T., Hidaka, M., Horibe, M., Mizushima, N., Yamamoto, N., Takahashi, T., Komiyama, M.: Predominant role of basicity of leaving group in α-effect for nucleophilic ester cleavage. Bioorg Chem **32**, 26–37 (2004)
13. Dixon, J.E., Bruice, T.C.: α-Effect. IV. Additional observation on the α-effect employing malachite green as substrate. J Am Chem Soc **93**, 6592–6597 (1971)
14. Wiberg, K.B.: The mechanisms of hydrogen peroxide reactions. II. A comparison of the reactivity of hydroxyl ion and hydroperoxide ion toward benzonitrile. J Am Chem Soc **77**, 2519–2521 (1955)
15. Buncel, E., Um, I.H.: The α-effect and its modulation by solvent. Tetrahedron **60**, 7801–7825 (2004)
16. Isolani, P.C., Riveros, J.M.: Energy-requirements for indirect formation of cluster ions in gas-phase ion–molecule reaction of negative ions with esters of formic-acid. Chem Phys Lett **33**, 362–364 (1975)
17. DePuy, C.H., Della, E.W., Filley, J., Grabowski, J.J., Bierbaum, V.M.: Absence of an α-effect in the gas phase nucleophilic reactions of HOO^-. J Am Chem Soc **105**, 2481–2482 (1983)
18. DePuy, C.H., Grabowski, J.J., Bierbaum, V.M., Ingemann, S., Nibbering, N.M.M.: Gas-phase reactions of anions with methyl formate and *N*,*N*-dimethylformamide. J Am Chem Soc **107**, 1093–1098 (1985)
19. Frink, B.T., Hadad, C.M.: Flowing afterglow study of the gas phase nucleophilic reactions of some formyl, acetyl, and cyclic esters. J Chem Soc Perkin Trans **2**, 2397–2407 (1999)
20. Garver, J.M., Yang, Z., Wehres, N., Nichols, C.M., Worker, B.B., Bierbaum, V.M.: The α-effect in elimination reactions and competing mechanisms in the gas phase. Int J Mass Spectrom **330**, 182–190 (2012)
21. Johlman, C.L., Wilkins, C.L.: Gas-phase reactions of nucleophiles with methyl formate. J Am Chem Soc **107**, 327–332 (1985)
22. Takashima, K., Riveros, J.M.: Gas-phase pathways for ester hydrolysis. J Am Chem Soc **100**, 6128–6132 (1978)
23. Patterson, E.V., Fountain, K.R.: On gas-phase α-effects. I. The gas-phase manifestation and potential SET character. J Org Chem **71**, 8121–8125 (2006)
24. McAnoy, A.M., Paine, M.R.L., Blanksby, S.J.: Reactions of the hydroperoxide anion with dimethyl methylphosphonate in an ion trap mass spectrometer: evidence for a gas-phase α-effect. Org Biomol Chem **6**, 2316–2326 (2008)
25. McAnoy, A.M., Williams, J., Paine, M.R.L., Rogers, M.L., Blanksby, S.J.: Ion–molecule reactions of *O*, *S*-dimethyl methylphosphonothioate: evidence for intramolecular sulfur oxidation during VX perhydrolysis. J Org Chem **74**, 9319–9327 (2009)
26. Thomsen, D.L., Reece, J.N., Nichols, C.M., Hammerum, S., Bierbaum, V.M.: Investigating the α-effect in gas-phase S_N2 reactions of microsolvated anions. J Am Chem Soc **135**, 15508–15514 (2013)
27. Thomsen, D.L., Reece, J.N., Nichols, C.M., Hammerum, S., Bierbaum, V.M.: The α-effect in gas-phase S_N2 reactions of microsolvated anions: methanol as a solvent. J Phys Chem A (2013). doi:10.1021/jp407698a
28. Van Doren, J.M., Barlow, S.E., DePuy, C.H., Bierbaum, V.M.: The tandem flowing afterglow-SIFT-drift. Int J Mass Spectrom Ion Process **81**, 85–100 (1987)
29. Bierbaum, V.M. In: *Encyclopedia of Mass Spectrometry*; Gross, M.L., Caprioli, R., Eds.; Vol. 1, Elsevier: Amsterdam, pp. 98–109 (2003)
30. Bickelhaupt, F.M., de Koning, L.J., Nibbering, N.M.M.: Anionic ether cleavage of tetrahydrofuran in the gas-phase. Tetrahedron **49**, 2077–2092 (1993)
31. Su, T., Chesnavich, W.J.: Parametrization of the Ion-Polar Molecule Collision Rate Constant by Trajectory Calculations. J Chem Phys **76**, 5183–5185 (1982)
32. Frisch, M.J., Trucks, G.W., Schlegel, H.B., Scuseria, G.E., Robb, M.A., Cheeseman, J.R., Scalmani, G., Barone, V., Mennucci, B., Petersson, G.A., Nakatsuji, H., Caricato, M., Li, X., Hratchian, H.P., Izmaylov, A.F., Bloino, J., Zheng, G., Sonnenberg, J.L., Hada, M., Ehara, M., Toyota, K., Fukuda, R., Hasegawa, J., Ishida, M., Nakajima, T., Honda, Y., Kitao, O., Nakai, H., Vreven, T., Montgomery, J.A., Jr., Peralta, J.E., Ogliaro, F., Bearpark, M., Heyd, J.J., Brothers, E., Kudin, K.N., Staroverov, V.N., Kobayashi, R., Normand, J., Raghavachari, K., Rendell, A., Burant, J.C., Iyengar, S.S., Tomasi, J., Cossi, M., Rega, N., Millam, N.J., Klene, M., Knox, J.E., Cross, J.B., Bakken, V., Adamo, C., Jaramillo, J., Gomperts, R., Stratmann, R.E., Yazyev, O., Austin, A.J., Cammi, R., Pomelli, C., Ochterski, J.W., Martin, R.L., Morokuma, K., Zakrzewski, V.G., Voth, G.A., Salvador, P., Dannenberg, J.J., Dapprich, S., Daniels, A.D., Farkas, Ö., Foresman, J.B., Ortiz, J.V., Cioslowski, J., Fox, D.J. Gaussian 09, Revision B.01. Gaussian, Inc, Wallingford (2010)
33. Ren, Y., Yamataka, H.: G2(+) Investigation on the α-effect in the S_N2 reactions at saturated carbon. Chem Eur J **13**, 677–682 (2007)
34. Glukhovtsev, M.N., Pross, A., Radom, L.: Gas-phase identity S_N2 reactions of halide anions with methyl halides—a high-level computational study. J Am Chem Soc **117**, 2024–2032 (1995)
35. Scott, A.P., Radom, L.: Harmonic vibrational frequencies: an evaluation of Hartree-Fock, Moller-Plesset, quadratic configuration interaction, density functional theory, and semiempirical scale factors. J Phys Chem **100**, 16502–16513 (1996)
36. Bohme, D.K., Mackay, G.I.: Bridging the gap between the gas-phase and solution: transition in the kinetics of nucleophilic displacement-reactions. J Am Chem Soc **103**, 978–979 (1981)
37. Bohme, D.K., Raksit, A.B.: Gas-phase measurements of the influence of stepwise solvation on the kinetics of nucleophilic displacement-reactions with CH_3Cl and CH_3Br at room-temperature. J Am Chem Soc **106**, 3447–3452 (1984)
38. Hierl, P.M., Ahrens, A.F., Henchman, M., Viggiano, A.A., Paulson, J.F., Clary, D.C.: Nucleophilic displacement as a function of hydration number and temperature: rate constants and product distribution for $OD^-(D_2O)_{0,1,2}+CH_3Cl$ at 200–500 K. J Am Chem Soc **108**, 3142–3143 (1986)
39. Hierl, P.M., Paulson, J.F., Henchman, M.J.: Translational energy-dependence of cross-sections for reactions of $OH^-(H_2O)_n$ with CH_3Cl and CH_3Br. J Phys Chem **99**, 15655–15661 (1995)
40. Seeley, J.V., Morris, R.A., Viggiano, A.A.: Temperature dependences of the rate constants and branching ratios for the reactions of $F^-(H_2O)_{(0-5)}$ with CH_3Br. J Phys Chem A **101**, 4598–4601 (1997)
41. Viggiano, A.A., Arnold, S.T., Morris, R.A., Ahrens, A.F., Hierl, P.M.: Temperature dependences of the rate constants and branching ratios for the reactions of $OH^-(H_2O)_{(0-4)}+CH_3Br$. J Phys Chem **100**, 14397–14402 (1996)
42. Pross, A., Shaik, S.S.: Reactivity–selectivity relationships. A quantum-mechanical approach to transition-state structure. application to the S_N2 reaction of benzyl derivatives. J Am Chem Soc **103**, 3702–3709 (1981)
43. Bordwell, F.G., Clemens, A.H.: Correlation between the basicity of carbanions and their ability to transfer an electron. J Org Chem **46**, 1035–1037 (1981)
44. Terrier, F., Mokhtari, M., Goumont, W., Halle, J.C., Buncel, E.: High Bronsted β_{nuc} values in S_NAr displacement. An indicator of the SET pathway? Org Biomol Chem **1**, 1757–1763 (2003)
45. Hoz, S.: The α-effect: on the origin of transition-state stabilization. J Org Chem **47**, 3545–3547 (1982)

46. Paranjothy, M., Sun, R., Zhuang, Y., Hase, W.L.: Direct chemical dynamics simulations: coupling of classical and quasiclassical trajectories with electronic structure theory. Wiley Interdisc Rev Comput Mol Sci **3**, 296–316 (2013)

47. Otto, R., Xie, J., Brox, J., Trippel, S., Stei, M., Best, T., Siebert, M.R., Hase, W.L., Wester, R.: Reaction dynamics of temperature-variable anion water clusters studied with crossed beams and by direct dynamics. Faraday Discuss **157**, 41–57 (2012)